Serra Alfonso, P.; Messmer, A.; Sanderson, D.; James, D.; Flores Pedauye, R. (2018). Apple hammerhead viroid-like RNA is a bona fide viroid: Autonomous replication and structural features support its inclusion as a new member in the genus Pelamoviroid. Virus Research. 249:8-15. https://doi.org/10.1016/j.virusres.2018.03.001

Title: Apple hammerhead viroid-like RNA is a *bona fide* viroid: autonomous replication and structural features support its inclusion as a new member in the genus *Pelamoviroid*

Authors: Pedro Serra, Amber Messmer, Daniel Sanderson, Delano James, Ricardo Flores

PII: S0168-1702(18)30049-2
DOI: https://doi.org/10.1016/j.virusres.2018.03.001
Reference: VIRUS 97353

To appear in: *Virus Research*

Received date: 24-1-2018
Revised date: 2-3-2018
Accepted date: 2-3-2018

Please cite this article as: Serra, Pedro, Messmer, Amber, Sanderson, Daniel, James, Delano, Flores, Ricardo, Apple hammerhead viroid-like RNA is a bona fide viroid: autonomous replication and structural features support its inclusion as a new member in the genus Pelamoviroid.Virus Research https://doi.org/10.1016/j.virusres.2018.03.001

Apple hammerhead viroid-like RNA is a *bona fide* viroid: autonomous replication and structural features support its inclusion as a new member in the genus *Pelamoviroid*

Pedro Serra [1], Amber Messmer [2], Daniel Sanderson [2], Delano James [2], Ricardo Flores [1]*

[1] *Instituto de Biologia Molecular y Celular de Plantas (UPV-CSIC), Universidad Politécnica de Valencia, Avenida de los Naranjos, 46022 Valencia, Spain*

[2] *Centre for Plant Health – Sidney Laboratory, Canadian Food Inspection Agency, 8801 East Saanich Road, North Saanich, British Columbia, V8L 1H3, Canada*

*Corresponding author. *E-mail address:* rflores@ibmcp.upv.es (R. Flores).

Highlights

- Apple hammerhead viroid (AHVd) RNA replicates autonomously: it is a *bona fide* viroid
- The conformation of the AHVd (+) strand is stabilized by a kissing-loop interaction
- This tertiary interaction also exists in the two known pelamoviroids
- AHVd fulfills the criteria to be assigned to genus *Pelamoviroid*, family *Avsunviroidae*
- Pelamoviroids display low global sequence identity but high structural conservation

ABSTRACT

Apple hammerhead viroid-like RNA (AHVd RNA) has been reported in different apple cultivars and geographic regions and, considering the presence of hammerhead ribozymes in both polarity strands, suspected to be either a viroid of the family *Avsunviroidae* or a viroid-like satellite RNA. Here we report that dimeric head-to-tail *in vitro* transcripts of a 433-nt reference variant of AHVd RNA from

cultivar "Pacific Gala" are infectious when mechanically inoculated to apple, thus showing that this RNA is a *bona fide* viroid for which we have kept the name apple hammerhead viroid (AHVd) until its pathogenicity, if any, is better assessed. By combining thermodynamics-based predictions with co-variation analyses of the natural genetic diversity found in AHVd we have inferred the most likely conformations for both AHVd polarity strands *in vivo*, with that of the (+) polarity strand being stabilized by a kissing loop-interaction similar to those reported in peach latent mosaic viroid and chrysathemum chlorotic mottle viroid, the two known members of the genus *Pelamoviroid* (family *Avsunviroidae).* Therefore, AHVd RNA fulfills the biological and molecular criteria to be allocated to this genus, the members of which, intriguingly, display low global sequence identity but high structural conservation.

Keywords:
Apple hammerhead viroid
Pelamoviroids
Kissing-loop interaction
Co-variation analysis

1. Introduction

Among the fundamental characteristics of viroids, small (~250-400 nt) non-protein-coding circular RNAs, is the ability to replicate autonomously and invade systemically their host plants, wherein they often incite disease (Diener et al., 2003; Flores et al., 2005; Tsagris et al., 2008; Ding 2010; Kovalskaya and Hammond, 2014; Palukaitis, 2014; Flores et al., 2015; Hadidi et al., 2017). Such an ability, which is indispensable to establish the viroid nature of a candidate RNA and eventually to fulfill Koch's postulates, is laborious to prove for those viroids whose natural hosts are woody species and lack experimental herbaceous hosts. This was the case for two of the four components of the family *Avsunviroidae,* including the type member avocado sunblotch viroid (ASBVd) (Symons, 1981) and peach latent mosaic viroid

(PLMVd) (Hernández and Flores, 1992), and remains still a challenge for two other circular RNAs identified by a combination of deep sequencing and bioinformatics tools: grapevine hammerhead viroid-like RNA (GHVd RNA) (Wu et al., 2012) and apple hammerhead viroid-like RNA (AHVd RNA) (Zhang et al., 2014). Mention of hammerhead in their provisional names refers to one typical feature of members of the family *Avsunviroidae:* the oligomeric strands of both polarities, resulting from replication in plastids through a symmetric rolling-circle mechanism (Branch and Robertson, 1984; Hutchins et al., 1985; Daròs et al., 1994; Flores et al., 2014), self-cleave via *cis*-acting hammerhead ribozymes (Hutchins et al., 1986) operating co-transcriptionally (Carbonell et al., 2006), into unit-length strands that are subsequently circularized. These ribozymes, formed by a central conserved core flanked by short helices capped by small loops (Prody et al., 1986; Forster and Symons, 1987a; Forster and Symons, 1987b; Ruffner et al. 1990; Flores et al., 2001; Martick and Scott, 2006), can be easily identified even by visual inspection of the corresponding sequences. However, the presence of hammerheads does not prove that an RNA is a viroid because such ribozymes have been found additionally in: i) viroid-like satellite RNAs that share some properties with viroids, including small size, lack of protein-coding ability and rolling-circle replication, but depend functionally on specific RNA viruses to complete their infectious cycle (Schneider, 1969; Randles et al., 1981; Symons and Randles, 1999), ii) two small circular RNAs from cherry, possibly also viroid-like satellite RNAs since they are found in strict association with a series of mycoviral double-stranded RNAs (Di Serio et al., 2006), and iii) a small circular RNA from carnation with a DNA counterpart, a so-called retroviroid-like element (Hernández et al., 1992; Daròs and Flores, 1995; Hegedus et al., 2001). More recently, hammerheads have been found encoded in a large number of genomes distributed ubiquitously along the tree of life (De la Peña and García-Robles, 2010; Hamman et al., 2012).

Since their discovery, GHVd RNA and AHVd RNA have retained the status of viroid-like RNAs because, despite some attempts, no proof of autonomous replication has been provided so far (Wu et al., 2012; Zhang et al., 2014; Messmer et al., 2017). Nevertheless, there is a good reason to consider that they could be true

viroids. The branched conformation of the PLMVd is stabilized by a kissing-loop interaction (Bussière et al., 2000) that was also predicted (Bussière et al., 2000) and then confirmed (Gago et al., 2005) in chrysanthemum chlorotic mottle viroid (CChMVd) (Navarro and Flores, 1997), in which it is essential for *in vitro* folding and *in vivo* viability (Gago et al., 2005). Such interaction exits only in the (+) strands of these two viroids (Gago et al., 2005; Dubé et al., 2010; Dubé et al., 2011; Giguère et al., 2014), which together form the genus *Pelamoviroid* (Navarro and Flores, 1997), thus establishing a structural and possibly functional difference with their corresponding (-) strands. Notably, a similar kissing-loop interaction has been predicted in the (+) strand of GHVd RNA (Wu et al., 2012), while two tentative interactions of this class have been proposed in the (+) strand of AHVd RNA (Zhang et al., 2014).

Here, using dimeric head-to-tail *in vitro* transcripts, we report that AHVd RNA is infectious in apple and, hence, a true viroid (the biggest in size reported excluding those with sequence repeats). Moreover, based on *in silico* predictions and on a co-variation study of the existing sequence variants of AHVd RNA, we have figured out the most likely conformations of both strands *in vivo* and mapped a kissing-loop interaction stabilizing that of (+) polarity. Therefore, AHVd RNA satisfies the criteria to be considered a new member of the genus *Pelamoviroid.*

2. Materials and methods

2.1. Source of infected material and bioassay

An RNA preparation from leaves of an AHVd-infected apple tree of cultivar "Pacific Gala" (Messmer et al., 2017), obtained with the RNeasy Plant Mini Kit (Qiagen), was reverse transcribed and PCR-amplified (see below) using the abutted primers RF-1385 and RF-1386 (Table 1). The full-length product was eluted from non-denaturing PAGE in 5% gels and ligated with T4 DNA ligase (Thermofisher), with the resulting dimer being identified by its size, gel-eluted, cloned in pBlueScript II KS+ (Stratagene) and checked for proper head-to-tail orientation and sequence. Young stems of small apple plants *(Malus pumila* M.) from four commercial cultivars

("Esperiega", "Granny", "Verde doncella" and "Brookfield") were slashed-inoculated with *in vitro* transcripts of a linearized recombinant plasmid containing an AHVd-cDNA dimeric insert of the 433-nt reference variant from "Pacific Gala" (GenBank MF402932) and kept in the greenhouse. Control plants of the same varieties were mock-inoculated with buffer (50 mM K_2HPO_4).

2.2. RNA extraction, partial purification, and analysis by non-denaturing and denaturing PAGE and gel-blot hybridization

Preparations enriched in RNAs with a high content in secondary structure from young expanding leaves of AHVd-infected apple trees, and from mock-inoculated controls, were obtained by extraction with buffer-saturated phenol and fractionation with non-ionic cellulose (CF11, Whatman), and resuspended in sterile deionized water. Aliquots were examined with double PAGE: after non-denaturing PAGE in a 5% gel in 1X TAE and staining with ethidium bromide, the segment delimited by the DNA markers of 300 and 500 bp (including the 371-nt citrus exocortis viroid, CEVd, serving as control) was cut and put on top of a single-well second denaturing 5% gel in 0.25X TBE and 8 M urea, in which the viroid circular forms display a slower electrophoretic mobility than their linear counterparts (Pallás et al., 1987). For preparative purposes, the AHVd circular forms were identified by ethidium bromide staining and eluted from the gel. For analytical purposes, the RNAs separated in the second denaturing gel were electrotransferred to positively-charged nylon membranes (Roche Diagnostics). After UV irradiation for fixing the RNAs, the membranes were hybridized with a digoxigenin-labeled full-length riboprobe for detecting the AHVd (+) strands prepared by transcription with T7 RNA polymerase (Thermofisher) (Sambrook et al., 1989) of the corresponding linearized recombinant plasmid.

2.3. RT-PCR amplification, cloning, and sequencing

Nucleic acid preparations enriched in AHVd RNAs, were subjected to reverse-

transcription (RT) at 42 °C for 45 min with Superscript II reverse transcriptase in the buffer recommended by the supplier (Invitrogen). The resulting cDNAs were PCR-amplified with *Pfu* DNA polymerase in the buffer recommended by the supplier (Agilent), by applying an initial denaturation at 95ºC for 2 min, followed by 30 amplification cycles (95 ºC for 30 s, 60 ºC for 30 s and 72ºC for 40 s). Primers for RT-PCR are indicated in Results and Table 1. The nucleotide sequence of the resulting RT-PCR products from AHVd, cloned in the *Eco*RV site of pBlueScript II KS+ (Stratagene), was determined with an ABI 3100 Genetic Analyzer (Applied Biosystems). Subsequently, unit-length AHVd-DNA products from certain variants were obtained by PCR-amplification with the same phosphorylated primer pairs, eluted following non-denaturing PAGE in 5% gels, and ligated with T4 DNA ligase. The dimeric AHVd-DNA products were again cloned in the *Eco*RV site of pBlueScript II KS+, with the inserts being sequenced to verify proper orientation, sequence and integrity. The corresponding dimeric plamids were linearized with *Xho*I or *Eco*RI and transcribed under standard conditions with T7 or T3 RNA polymerases (Thermofisher), respectively (Sambrook et al., 1989). To increase the self-cleavage yield during transcription, recombinant plasmids containing dimeric AHVd-DNA inserts were prepared following the same approach but with the phosphorylated primers RF-1422 and RF-1423 (Table 1).

2.4. Site-directed mutagenesis

The dimeric plasmid containing the head-to-tail cDNA of the 433-nt AHVd reference variant from cultivar "Pacific Gala" (GenBank MF402932) served for PCR amplification using pairs of adjacent and phosphorylated primers, complementary and homologous to the AHVd cDNA sequence except in 5'-proximal positions where changes were introduced to obtain the desired single mutants disrupting the kissing-loop interaction (see Results and Table 1). The double mutant restoring this tertiary interaction was constructed from one of the single mutants following essentially the same procedure. The PCR cycling profile was as detailed above. Cloning and sequencing confirmed that the new plasmid inserts contained only the expected

mutations. The corresponding dimeric transcripts were generated as indicated above. The resulting products were separated by denaturing PAGE in 1X TBE and 8 M urea, and the unit-length segments generated by self-cleavage during *in vitro* transcription were eluted and their mobilities examined by non-denaturing PAGE.

2.5. Sequence comparisons and prediction of RNA secondary structure

Pairwise alignments were performed with the software program MUSCLE (Edgar, 2004a; Edgar, 2004b). The secondary structures of minimal free energy at 37 °C of AHVd (+) and (-) strands were predicted with the *RNAfold* software program included in the ViennaRNA package version 2.4.1 (Lorenz et al., 2011), using the circular version and default parameters. These structures were manually refined according to results of co-variation analyses of the natural AHVd genetic diversity.

3. Results

3.1. Dimeric head-to-tail in vitro transcripts of AHVd RNA are infectious in apple

We first subjected to RT-PCR amplification a nucleic acid preparation from a Canadian apple tree of cultivar "Pacific Gala" that tested positive for AHVd RNA (Messmer et al., 2017). The 433-nt reference sequence of this isolate (GenBank MF402932) differed from the 434-nt reference sequence (GenBank KR506605) of cultivar "Fuji" reported in China (Zhang et al., 2014) in 62 positions (14%), including three indels. Although some of the changes observed in the "Pacific Gala" reference variant mapped at the hammerheads, they did not affect the critical elements of these ribozymes (see below) and, consequently, their self-cleavage activity *in vitro* (Fig. 1), in line with previous observations made with the "Fuji" reference variant (Zhang et al., 2014). To reassess the sequence diversity of the "Pacific Gala" isolate we designed the abutted primers RF-1379 and RF-1380, degenerated in three positions (Table 1), so that they could amplify variants observed in both cultivars. However, RT-PCR, cloning and sequencing of 15 full-length clones revealed that all variants were

essentially identical to the reference sequence of "Pacific Gala" (Supplementary Fig. S1). From this sequence we then designed a second pair of abutted primers, RF-1385 and RF-1386 (Table 1), to confirm the sequence of the region covered by the first primer pair. RT-PCR, cloning and sequencing of another set of 15 full-length clones failed to detect any variability in that region (Supplementary Fig. S2), thus corroborating the low genetic diversity of the "Pacific Gala" isolate examined (Messmer et al., 2017).

To test the potential infectivity of the reference variant of the "Pacific Gala" AHVd RNA, dimeric head-to-tail *in vitro* transcripts were mechanically inoculated by slashing young stems of two apple plants of four different apple varieties (n=8), with additional mock-inoculated plants of each variety serving as controls. After four months in the greenhouse, upper leaves emerged in the inoculated stems were collected and processed, and nucleic acid preparations enriched in viroid-like RNAs (Pallás et al., 1987) were separated by double polyacrylamide gel electrophoresis (PAGE), first under non-denaturing and then under denaturing conditions, and examined by RNA gel-blot hybridization with a full-length digoxigenin-labeled riboprobe for detecting AHVd RNA (+) strands. Bands with the mobility expected for the circular and linear AHVd RNA forms (the first migrating more slowly than the 371-nt circular form of CEVd, used as control), were observed in the two inoculated plants of variety V1 and in one of the two inoculated plants of variety V2, but not in the mock-inoculated plants (Fig. 2). To further validate that these bands were indeed generated by AHVd RNA replicating *de novo*, the corresponding RNA preparations were subjected to RT-PCR with primers RF-1385 and RF-1386, and the DNA products of the expected size were cloned and sequenced. The 15 clones (five from each plant) showed the same sequence as the parental variant. Altogether these results showed that the AHVd RNA is indeed a viroid endowed with autonomous replication and movement, to which hereafter we will refer as apple hammerhead viroid (AHVd).

3.2. Co-variation analysis leads to well-supported in vivo conformations for the (+) and (-) strands of AHVd RNA

Determining a reliable secondary structure for the (+) strand of AHVd RNA *in planta* was critical for the further search of stabilizing elements of tertiary structure, particularly kissing-loop interactions, as those reported in other viroids (Bussière et al., 2000; Gago et al., 2005). For this objective, we first obtained the most stable secondary structure predicted with the *RNAfold* software program (Lorenz et al., 2011), applying this tool to the full-length AHVd (+) RNA of the reference variants of cultivars "Pacific Gala" and "Fuji" (GenBank MF402932 and KR506605, respectively) and to portions thereof. In line with previous predictions *in silico* (Zhang et al., 2014; Messmer et al., 2017), the resulting conformations were composed by a rod-like domain (containing the nucleotides forming the hammerhead structures) essentially common to both variants, and by a multi-branched domain showing some differences between variants. To solve this issue and produce a conformation that could potentially accommodate the sequence diversity existing in the two reference variants and in others reported previously (Zhang et al., 2014; Messmer et al., 2017) as well as in the present work, we validated the individual hairpins when the sequence variability resulted in co-variations (and conversions of canonical into wobble base-pairs, or vice versa) that did not disrupt the corresponding stems or mapped at the loops.

Because the natural sequence diversity between the AHVd isolates of different cultivars and geographic origin is relatively high, this *in vivo* approach indeed resulted in reliable conformations. Focusing first on that of the AHVd (+) strand (Fig. 3), and more specifically in the rod-like domain containing the nucleotides forming the hammerheads: i) the stem delimited by positions 66-73 and 84-91 is well-supported by six co-variations, ii) the stem delimited by positions 53-60 and 108-115 is also supported by four conversions of canonical into wobble base-pairs, and iii) the stem delimited by positions 46-122 and 48-120 is likewise supported by one co-variation and two conversions of canonical into wobble base-pairs. All these substitutions do not disrupt the corresponding stems, with most of the remaining changes mapping at loops. Regarding the substitutions located in both hammerheads, they result either in the conversion of canonical into wobble base-

pairs or vice versa, or they map at loops (Fig. 3, inset 1), hence not affecting the thermodynamic stability of the ribozymes and, consequently, their catalytic activity (Fig. 1). Finding a consistent conformation for the multi-branched domain was more difficult, but essentially all the stems of the proposed folding (Fig. 3) are supported by co-variations or conversions of canonical into wobble base-pairs, or vice versa; see for instance: i) the stem delimited by positions 272-280 and 285-293, which is supported by four co-variations maintaining three consecutive base-pairs, and one substitution converting a canonical into a wobble base-pair, and ii) the stem delimited by positions 317-328 and 395-407, which is supported by two co-variations and one substitution converting a canonical into a wobble base-pair. The preservation and relevance of the stem delimited by positions 329-338 and 353-361 is discussed below.

Regarding the conformation of the AHVd (-) strand, the central part of the rod-like domain is very similar to that of the (+) strand because, in both cases, most of the nucleotides forming the central conserved core and adjacent helices of the two hammerheads are base-paired. The left part of the rod-like domain is also very similar to that of the (+) strand: the stem delimited by positions 66-73 and 84-91 is supported by several co-variations and flanked by a loop and a bulge of 10- and 11-nt, respectively (Supplementary Fig. S3). As indicated above, the substitutions located in the (-) hammerhead do not disrupt the helices flaking the central conserved core or map at one loop (Fig. 3, inset 1), thus not affecting the catalytic activity of the ribozyme (Fig. 1). The natural variability also supports some of the stems of the multi-branched domain proposed for the AHVd (-) strand, the most prominent of which are those delimited by positions 270-279 and 286-294 (supported by four co-variations in three consecutive base-pairs and one substitution converting a wobble into a canonical base-pair) (Supplementary Fig. S3), and by positions 328-333 and 341-346 (with four consecutive substitutions leading to a slight rearrangement) (Supplementary Fig. S3, inset 2).

3.3. Evidence underpinning the existence of a kissing-loop interaction stabilizing the branched conformation of the AHVd (+) strand

Given the structural similarities between the (+) strands of PLMVd, CChMVd and AHVd, reflected in a rod-like/cruciform domain —comprising the nucleotides forming the hammerhead structures— merged to a multi-branched domain, we next examined whether this latter domain was stabilized in AHVd by a kissing-loop interaction similar to those reported previously in PLMVd (Bussière et al., 2000) and CChMVd (Gago et al., 2005). Visual inspection of the proposed secondary structure revealed the possibility of such tertiary interaction between nucleotides at positions 304-307 (GUCG) and 345-348 (UGAC) (Fig. 3). Evidence supporting this possibility includes: i) an A→G substitution (position 347) found in one natural variant that results in the conversion of a canonical into a wobble pair, and ii) three co-variations and one substitution converting a canonical into a wobble base-pair in the stem (delimited by positions 329-338 and 353-361) capped by one of the interacting loops (Fig. 3); interestingly, in the reference variant of cultivar "Fuji" three of the substitutions (positions U333, C334 and A357) induce a slight rearrangement of the stem that leaves C334 unpaired (Fig. 3, inset 2). Preservation of this stem —with an unpaired nucleotide at position 333 or 334 that possibly causes a bend— is indicative of its relevance in keeping the close proximity and proper orientation between the two kissing loops. Analysis of the genetic heterogeneity of additional AHVd isolates should hopefully provide further *in vivo* support for the proposed kissing-loop interaction or a variation thereof. Notably, examination of the AHVd (-) strand failed to disclose any similar element of tertiary structure (Supplementary Fig. 3), thus bolstering the view that the kissing-loop interaction is restricted to the AHVd (+) strand, as in PLMVd (Bussière et al., 2000; Dubé et al., 2010) and CChMVd (Gago et al., 2005).

To make a stronger case for the physical existence of such a kissing-loop interaction, we applied the same strategy developed previously for CChMVd (Gago et al., 2005): using primers RF-1388 and RF-1389, and RF-1390 and RF-1391 (Table 1), the four contiguous nucleotides of each loop involved in the interaction were interchanged, generating an AHVd variant with eight mutations (GUCG304-307→UGAC and UGAC345-348→GUCG), in which an alternative, but energetically

similar, kissing-loop interaction could be adopted. The two quadruple mutants (GUCG304-307→UGAC) and (UGAC345-348→GUCG), wherein the kissing-loop interaction was disrupted, and the wild-type variant served as controls. The corresponding dimeric head-to-tail cDNAs were inserted into a transcription vector, and the monomeric self-cleavage products generated during *in vitro* transcriptions of the primary dimeric AHVd (+) RNAs were eluted from denaturing PAGE in a 5% gel. In subsequent examination by non-denaturing PAGE in a 5% gel, the four monomeric RNAs displayed indistinguishable mobility (data not shown), while we anticipated a slower mobility for the two quadruple mutants in which disruption of the kissing-loop interaction should result in a less compact conformation. Further analyses by non-denaturing PAGE in gels of lower porosity (8%) and co-electrophoresis of mixed samples, failed to disclose any reproducible difference, as also failed addition of magnesium to the samples (data not shown). Possible reasons for these observations include: i) the larger size of AHVd with respect to PLMVd and CChMVd, which could mask the minor differences in mobility induced by the presence or absence of the kissing-loop interaction, and ii) the lack of predominant conformations for the wild-type and mutated AHVd (+) RNAs when folded *in vitro*, as suggested by the rather diffuse appearance of the corresponding gel bands; as highlighted before (Uhlenbeck, 1995; López-Carrasco et al., 2016), conformations adopted *in vitro* do not necessarily reflect those existing *in vivo*. On the other hand, when the AHVd (+) and (-) monomeric RNAs were compared by non-denaturing PAGE in 5% gels, a distinction was detected, with the former moving faster than the latter, and both migrating as blurred bands (Fig. 4).

In addition to the kissing-loop interaction described above, we have observed another potential long-distance interaction in the AHVd (+) strand between nucleotides at positions 96-100 and 213-217 (forming part of a bulge and a hairpin loop, respectively) (Fig. 3). Similar interactions, although between two hairpin loops, have been proposed previously from co-variation analysis (Ambrós et al., 1998) and selective 2'-hydroxyl acylation analyzed by primer extension *in vitro* (Dubé et al., 2011) in the PLMVd (+) strand, but not in the CChMVd (+) strand (Gago et al., 2005; Giguère et al. 2014).

3.4. Genetic distance and biological properties support creation of a new species for AHVd

At present, an arbitrary level of less than 90% sequence identity throughout the whole genome and different biological properties, principally host range and symptoms, serve to create new viroid species (Owens et al., 2012; Di Serio et al., 2014). The sequence identity of AHVd (GenBank MF402932) in pairwise alignments with other hammerhead viroids, namely the members of the family *Avsunviroidae* excluding ASBVd because its small size (246-250 nt) makes unreliable this analysis, is considerably lower: 61% with PLMVd, 63.5% with CChMVd, and 57.8% with ELVd. Although the AHVd variants from cultivars "Fuji" (Zhang et al., 2014) and "Pacific Gala" cluster in distinct phylogenetically groups (Messmer et al., 2017), with the reference variants of both groups having just 86% sequence identity, we consider them as variants of the same viroid (and we anticipate the infectivity of that from cultivar "Fuji") because most of the sequence diversity detected does not affect a common global conformation, which is the trait specifically "seen" by the replication and trafficking machinery of the host leading ultimately to the systemic spread of the viroid. Moreover, these AHVd variants have been so far recovered only from a common host (apple). Because members of the family *Avsunviroidae* have a host range limited to their natural hosts and, occasionally, to a few related species, it seems unlikely that AHVd may infect additional hosts other than apple and close relatives. Therefore, the available evidence favors the creation of a new species, *Apple hammerhead viroid*, to be included in the genus *Pelamoviroid* of the family *Avsunviroidae* (see below).

4. Discussion

Establishing the viroid nature of a candidate small circular RNA is an important step for the ultimate goal of delineating the features that endow an RNA with independent replication, local and long-distance trafficking and, frequently, induction of symptoms in a susceptible host. Because the search for herbaceous

experimental hosts is an empirical and in many instances unsuccessful approach, and because no such hosts have been identified for those members of the family *Avsunviroidae* that infect woody plants naturally, we performed our infectivity bioassays directly in apple plants by inoculating mechanically dimeric transcripts of the AHVd dominant 433-nt variant of a "Pacific Gala" isolate. Our results show that AHVd is indeed a viroid endowed with autonomous replication and systemic spread. Even if this RNA has been found in some naturally-infected "Pacific Gala" apple trees displaying swelling and radial limb cracking (Messmer et al., 2017), a causal relationship is not yet evident. In support of this view, no specific symptoms have been observed in "Fuji" apple trees infected naturally (Zhang et al., 2014), or in greenhouse apple plants infected experimentally with AHVd (this work). Thus, we prefer to keep the name apple hammerhead viroid (AHVd) until its biological properties become better defined.

Considering the presence of hammerhead ribozymes in both polarity strands, the key taxonomic criterion for members of the family *Avsunviroidae* (Di Serio et al., 2014), AHVd should be allocated to this family. In agreement with this notion, AHVd lacks the central conserved region characteristic of members of the family *Pospiviroidae* (McInnes and Symons, 1991; Flores et al., 2012; Di Serio et al., 2014; Steger and Perreault, 2016). The morphology and thermodynamic stability of the AHVd hammerheads resemble those of PLMVd and CChMVd (genus *Pelamoviroid)* and eggplant latent viroid (ELVd) (genus *Elaviroid)* (Fadda et al., 2003), while they differ notably from those of ASBVd (genus *Avsunviroid)*.

In addition to hammerhead architecture, determining a reliable conformation is very important when it comes to genus assignment. For this purpose, predictions *in silico* of the most stable secondary structures were combined with analyses of co-variations, because their occurrence in natural variants, as opposed to the corresponding single substitutions, highlights the role of selection in purging *in vivo* non-viable variants due to disruption of specific stems (Gutell et al., 1994; Uhlenbeck, 1995; Cech, 2015; López-Carrasco et al., 2016). Conversions of canonical into wobble pairs or vice versa, are also very useful in this same context. The resulting global conformation of the AHVd (+) strand is composed of a rod-like domain containing

the nucleotides forming the hammerhead structures joined to a multi-branched domain most likely stabilized by a kissing-loop interaction. Such a global conformation and the element of tertiary structure, which have been previously reported in PLMVd and CChMVd (Bussière et al., 2000; Gago et al., 2005), strongly support the classification of AHVd along with these two viroids in the genus *Pelamoviroid.* This line of argument further upholds the view that GHVd RNA most likely also is a pelamoviroid. Moreover, as noted before (Wu et al., 2012; Zhang et al., 2014), while the most abundant viroid-derived small RNAs (vd-sRNAs) generated by the host RNA silencing machinery are of 21 and 22 nt (accompanied by significant levels of the 24-nt species) in plants infected by potato spindle tuber viroid and other members of the family *Pospiviroidae* that replicate in the nucleus through an asymmetric rolling-circle mechanism (Machida et al., 2007; Navarro et al., 2009; Di Serio et al., 2010; Martínez et al., 2010; Wang et al., 2011; Zhang et al., 2014), the vd-sRNAs of 21 nt clearly predominate (being those of 24 nt very minor) in plants infected by PLMVd (Di Serio et al. 2009; Bolduc et al., 2010; Navarro et al., 2012) and CChMVd (our unpublished data). Notably, the vd-sRNAs of 21 nt also prevail in apple infected by AHVd (Zhang et al., 2014) and in grapevine infected by GHVd (Wu et al., 2012), thus adding further credence that this is a general feature of pelamoviroids and that GHVd RNA belongs presumably to this group.

Since apple cultivars are vegetatively propagated, the genetic diversity observed for AHVd most likely comes from the independent evolution under the distinct pressures imposed by the different cultivars, geographic areas and agronomic practices. Last but not least, the present study reveals a striking feature that appears common to pelamoviroids: they display low sequence identity but high structural conservation including a kissing-loop interaction in their (+) strands. How operates this element of tertiary structure, which has been examined in detail *in vitro* and *in vivo* in CChMVd and found to be critical for infectivity (Gago et al., 2005), remains an intriguing conundrum.

Conflict-of-interest statement

The authors declare no conflict of interest.

Acknowledgements

We wish to express our gratitude to Dr. Marcos de la Peña for valuable suggestions, to María Pedrote for excellent technical assistance, and to Dr. Miguel Cambra for facilitating access to the apple material. This research was partly funded by grant BFU2014-56812-P (to R.F.) from the Ministerio de Economía y Competitividad (MINECO) of Spain (which included a posdoctoral contract for P.S.), and by the Canadian Food Inspection Agency's Plant Research and Strategies Technology Development (TD) Program (to D.J.).

REFERENCES

Ambrós, S., Hernández, C., Desvignes, J.C., Flores, R., 1998. Genomic structure of three phenotypically different isolates of peach latent mosaic viroid: implications of the existence of constraints limiting the heterogeneity of viroid quasi-species. J. Virol. 72, 7397–7406.

Bolduc, F., Hoareau, C., St-Pierre, P., Perreault, J.P., 2010. In-depth sequencing of the siRNAs associated with peach latent mosaic viroid infection. BMC Mol. Biol. 11, 16.

Branch, A.D., Robertson, H.D., 1984. A replication cycle for viroids and other small infectious RNAs. Science 223, 450-454.

Bussière, F., Ouellet, J., Côté, F., Lévesque, D., Perreault, J.P., 2000. Mapping in solution shows the peach latent mosaic viroid to possess a new pseudoknot in a complex, branched secondary structure. J. Virol. 74, 2647-2654.

Carbonell, A., De la Peña, M., Flores, R., Gago, S., 2006. Effects of the trinucleotide preceding the self-cleavage site on eggplant latent viroid hammerheads: differences in co- and post-transcriptional self-cleavage may explain the lack of trinucleotide AUC in most natural hammerheads. *Nucleic Acids Res*. 34, 5613-5622.

Cech, T.R., 2015. RNA World research-still evolving. RNA 21, 474-475.

Daròs, J.A., Marcos, J.F., Hernández, C., Flores, R., 1994. Replication of avocado sunblotch viroid: evidence for a symmetric pathway with two rolling circles and hammerhead ribozyme processing. Proc. Natl. Acad. Sci. USA 91, 12813-12817.

Daròs, J.A., Flores, R., 1995. Identification of a retroviroid-like element from plants. Proc. Natl. Acad. Sci. USA 92, 6856-6860.

De la Peña, M., García-Robles, I., 2010. Ubiquitous presence of the hammerhead ribozyme motif along the tree of life. RNA 16, 1943-1950.

Ding, B., 2010. Viroids: self-replicating, mobile, and fast-evolving noncoding regulatory RNAs. Wiley Interdiscip. Rev. RNA 1, 362-375.

Diener, T.O., 2003. Discovering viroids—a personal perspective. Nature Rev. Microbiol. 1, 75-80.

Di Serio, F., Daròs, J.A., Ragozzino, A., Flores, R., 2006. Close structural relationship between two hammerhead viroid-like RNAs associated with cherry chlorotic rusty spot disease. Arch. Virol. 151, 1539-1549.

Di Serio, F., Gisel, A., Navarro, B., Delgado, S., Martínez de Alba, A.E., Donvito, G., Flores, R., 2009. Deep sequencing of the small RNAs derived from two symptomatic variants of a chloroplastic viroid: implications for their genesis and for pathogenesis. PLoS One 4, e7539.

Di Serio, F., Martínez de Alba, A.E., Navarro, B., Gisel, A., Flores, R., 2010. RNA-dependent RNA polymerase 6 delays accumulation and precludes meristem invasion of a viroid that replicates in the nucleus. J. Virol. 84, 2477-2489.

Di Serio, F., Flores, R., Verhoeven, J.T., Li, S.F., Pallás, V., Randles, J.W., Sano, T., Vidalakis, G., Owens, R.A., 2014**.** Current status of viroid taxonomy. Arch. Virol. 159, 3467-3478.

Dubé, A., Baumstark, T., Bisaillon, M., Perreault, J.P., 2010. The RNA strands of the plus and minus polarities of peach latent mosaic viroid fold into different structures. RNA 16, 463-473.

Dubé, A., Bolduc, F., Bisaillon, M., Perreault, J.P., 2011. Mapping studies of the peach latent mosaic viroid reveal novel structural features. Mol. Plant Pathol. 12, 688-701.

Edgar, R.C., 2004. MUSCLE: multiple sequence alignment with high accuracy and high throughput. Nucleic Acids Res. 32, 1792-1797.

Edgar, R.C., 2004. MUSCLE: a multiple sequence alignment method with reduced time and space complexity. BMC Bioinformatics 5, 113.

Fadda, Z, Daròs, J.A., Fagoaga, C., Flores, R., Duran-Vila, N., 2003. Eggplant latent viroid (ELVd): candidate type species for a new genus within family *Avsunviroidae* (hammerhead viroids). J. Virol. 77, 6528-6532.

Flores, R., Hernández, C., de la Peña, M., Vera, A., Daròs, J.A., 2001. Hammerhead ribozyme structure and function in plant RNA replication. Methods Enzymol. 341, 540-552.

Flores, R., Hernández, C., Martínez de Alba, E., Daròs, J.A., Di Serio, F., 2005. Viroids and viroid-host interactions. Annu. Rev. Phytopathol. 43, 117-139.

Flores, R., Serra, P., Minoia, S., Di Serio, F., Navarro, B., 2012. Viroids: from genotype to phenotype just relying on RNA sequence and structural motifs. Front. Microbiol. 3, 217.

Flores, R., Gago-Zachert, S., Serra, P., Sanjuán, R., Elena, S.F., 2014. Viroids: survivors from the RNA world? Annu. Rev. Microbiol. 68, 395-414.

Flores, R., Minoia, S., Carbonell, A., Gisel, A., Delgado, S., López-Carrasco, A., Navarro, B., Di Serio, F., 2015. Viroids, the simplest RNA replicons: how they manipulate their hosts for being propagated and how their hosts react for containing the infection. Virus Res. 209, 136-145.

Forster, A.C., Symons, R.H., 1987a. Self-cleavage of plus and minus RNAs of a virusoid and a structural model for the active sites. Cell 49, 211-220.

Forster, A.C., Symons, R.H., 1987b. Self-cleavage of virusoid RNA is performed by the proposed 55-nucleotide active site. Cell 50, 9-16.

Gago, S., De la Peña, M., Flores, R., 2005. A kissing-loop interaction in a hammerhead viroid RNA critical for its *in vitro* folding and *in vivo* viability. *RNA* 11, 1073-1083.

Giguère, T., Adkar-Purushothama, C.R., Bolduc, F., Perreault, J.P., 2014. Elucidation of the structures of all members of the Avsunviroidae family. Mol. Plant Pathol. 15, 767-779.

Gutell, R.R., Larsen, N., Woese, C.R., 1994. Lessons from an evolving rRNA: 16S and 23S rRNA structures from a comparative perspective. Microbiol. Rev. 58, 10-26.

Hadidi, A., Flores, R., Randles, J.W., Palukaitis, P., (Eds.), 2017. Viroids and Satellites, Elsevier/Academic Press, London.

Hammann, C., Luptak, A., Perreault, J., De la Peña, M., 2012. The ubiquitous hammerhead ribozyme. RNA 18, 871-85.

Hegedus, K., Palkovics, L., Tóth, E.K., Dallmann, G., Balázs, E., 2001. The DNA form of a retroviroid-like element characterized in cultivated carnation species. J. Gen. Virol. 82, 687-691.

Hernández, C., Flores, R., 1992. Plus and minus RNAs of peach latent mosaic viroid self-cleave *in vitro* via hammerhead structures. Proc. Natl. Acad. Sci. USA 89, 3711-3715.

Hernández, C., Daròs, J.A., Elena, S.F., Moya, A., Flores, R., 1992. The strands of both polarities of a small circular RNA from carnation self-cleave in vitro through alternative double- and single-hammerhead structures. Nucleic Acids Res. 20, 6323-6329.

Hutchins, C.J., Keese, P., Visvader, J.E., Rathjen, P.D., McInnes, J.L., Symons, R.H., 1985. Comparison of multimeric plus and minus forms of viroids and virusoids. Plant Mol. Biol. 4, 293-304.

Hutchins, C., Rathjen, P.D., Forster, A.C., Symons, R.H. 1986. Self-cleavage of plus and minus RNA transcripts of avocado sunblotch viroid. Nucleic Acids Res. 14, 3627-3640.

Kovalskaya, N., Hammond, R.W., 2014. Molecular biology of viroid-host interactions and disease control strategies. Plant Sci. 228, 48-60.

Lorenz, R., Bernhart, S.H., Höner Zu Siederdissen, C., Tafer, H., Flamm, C., Stadler, P.F., Hofacker, I.L., 2011. ViennaRNA package 2.0. Algorithms Mol. Biol. 6, 26.

López-Carrasco, A., Gago-Zachert, S., Mileti, G., Minoia, S., Flores, R., Delgado, S., 2016. The transcription initiation sites of eggplant latent viroid strands map within distinct motifs in their *in vivo* RNA conformations. RNA Biol. 13, 83-97.

McInnes, J.L., Symons, R.H., 1991. Comparative structure of viroids and their rapid detection using radioactive and nonradioactive nucleic acid probes, in Maramorosch, K. (Ed.), Viroids and Satellites: Molecular Parasites at the Frontier of Life. CRC Press, Boca Raton, FL, pp. 21-58.

Machida, S., Yamahata, N., Watanuki, H., Owens, R., Sano, T., 2007. Successive accumulation of two size classes of viroid-specific small RNA in potato spindle tuber viroid-infected tomato plants. J. Gen. Virol. 88, 3452-3457.

Martick, M., Scott, W.G., 2006. Tertiary contacts distant from the active site prime a ribozyme for catalysis. Cell 126, 309-320.

Martínez, G., Donaire, L., Llave, C., Pallás, V., Gómez, G., 2010. High-throughput sequencing of hop stunt viroid-derived small RNAs from cucumber leaves and phloem. Mol. Plant Pathol. 11, 347-359.

Messmer, A., Sanderson, D., Braun, G., Serra, P., Flores, R., James, D., 2017. Molecular and phylogenetic identification of unique isolates of hammerhead

viroid-like RNA from 'Pacific Gala' apple *(Malus domestica)* in Canada. Can. J. Plant Pathol. 39, 342-353.

Navarro, B., Flores, R., 1997. Chrysanthemum chlorotic mottle viroid: unusual structural properties of a subgroup of viroids with hammerhead ribozymes. Proc. Natl. Acad. Sci. USA 94, 11262-11267.

Navarro, B., Pantaleo, V., Gisel, A., Moxon, S., Dalmay, T., Bisztray, G., Di Serio, F., Burgyán, J., 2009. Deep sequencing of viroid-derived small RNAs from grapevine provides new insights on the role of RNA silencing in plant-viroid interaction. PLoS One 4, e7686.

Navarro, B., Gisel, A., Rodio, M.E., Delgado, S., Flores, R., Di Serio, F., 2012. Small RNAs containing the pathogenic determinant of a chloroplast-replicating viroid guide the degradation of a host mRNA as predicted by RNA silencing. Plant J. 70, 991-1003.

Owens, R.A., Flores, R., Di Serio, F., Li, S.F., Pallás, V., Randles, J.W., Sano, T., Vidalakis, G. 2012. Viroids, in: King, A.M.Q., Adams, M.J., Carstens, E.B., Lefkowitz, E.J., (Eds.), Virus Taxonomy: Ninth Report of the International Committee on Taxonomy of Viruses. Elsevier/Academic Press, London, pp. 1221-1234.

Pallás, V., Navarro, A., Flores, R., 1987. Isolation of a viroid-like RNA from hop different from hop stunt viroid. J. Gen. Virol. 68, 3201-3205.

Palukaitis, P., 2014. What has been happening with viroids? Virus Genes 49, 175-184.

Prody, G.A., Bakos, J.T., Buzayan, J.M., Schneider, I.R., Bruening, G**.,** 1986. Autolytic processing of dimeric plant virus satellite RNA. Science 231, 1577-1580.

Randles, J.W., Davies, C., Hatta, T., Gould, A.R., Francki, R.I.B., 1981. Studies on encapsidated viroid-like RNA I. Characterization of velvet tobacco mottle virus. Virology 108, 111-122.

Ruffner, D.E., Stormo, G.D., Uhlenbeck, O.C., 1990. Sequence requirements of the hammerhead RNA self-cleavage reaction. Biochemistry 29, 10695-10702.

Sambrook, J., Fritsch, E.F., Maniatis, T., 1989. Molecular Cloning: a Laboratory Manual, second ed. Cold Spring Harbor Laboratory, Cold Spring Harbor, New York.

Schneider, I.R., 1969. Satellite-like particle of tobacco ringspot virus that resembles tobacco ringspot virus. Science 166,1627-1629.

Steger, G., Perreault, J.P., 2016. Structure and associated biological functions of viroids. Adv. Virus Res. 94, 141-172.

Symons, R.H., 1981. Avocado sunblotch viroid: primary sequence and proposed secondary structure. Nucleic Acids Res. 9, 6527-6537.

Symons, R.H., Randles, J.W., 1999. Encapsidated circular viroid-like satellite RNAs (virusoids) of plants. Curr. Top. Microbiol. Immunol. 239, 81-105.

Tsagris, E.M., Martínez de Alba, A.E., Gozmanova, M., Kalantidis, K., 2008. Viroids. Cell Microbiol. 10, 2168-2179.

Uhlenbeck, O.C., 1995. Keeping RNA happy. *RNA* 1, 4-6.

Wu, Q.F., Wang, Y., Cao, M.J., Pantaleo, V., Burgyan, J., Li, W.X., Ding, S.W., 2012. Homology-independent discovery of replicating pathogenic circular RNAs by deep sequencing and a new computational algorithm. Proc. Natl. Acad. Sci. USA 109, 3938-3943.

Wang, Y., Shibuya, M., Taneda, A., Kurauchi, T., Senda, M., Owens, R.A., Sano, T., 2011. Accumulation of potato spindle tuber viroid-specific small RNAs is accompanied by specific changes in gene expression in two tomato cultivars. Virology 413, 72-83.

Zhang, Z., Qi, S., Tang, N., Zhang, X., Chen, S., Zhu, P., Ma, L., Cheng, J., Xu, Y., Lu, M., Wang, H., Ding, S.W., Li, S., Wu, Q., 2014. Discovery of replicating circular RNAs by RNA-seq and computational algorithms. PLoS Pathog. 10, e1004553.

LEGENDS TO FIGURES

Fig. 1. (A) Schematic representation of the dimeric AHVd (+) and (-) transcripts and their expected self-cleavage products of the "Pacific Gala"reference variant (GenBank MF402932). Vector and viroid sequences are denoted by black and white bars, respectively, and the ribozyme (RZ) self-cleavage sites are marked by arrowheads. Numbers on the right indicate sizes (in nt). The (+) and (-) transcripts start at positions 90 and 89, respectively (the same numbering is used in both strands). (B) PAGE analysis in a 5% denaturing gel of the (+) and (-) in *vitro* transcription products of linearized plasmids containing head-to-tail dimeric AHVd-DNA inserts. M refers to RNA markers with their sizes on the left. The gel was stained with ethidium bromide.

Fig. 2. Analysis by double PAGE of apple plants inoculated with AHVd dimeric head-to-tail *in vitro* transcripts of the "Pacific Gala" reference variant (GenBank MF402932). (A) Ethidium bromide staining of the first non-denaturing gel showing the RNA levels of the different preparations enriched in viroid-like RNAs. Multimeric (100-bp DNA) size markers were applied to the two external lanes; the most intense band corresponds to 500 bp. (a), (b) and (c) indicate positions of CEVd, 5S rRNA and 4S tRNAs RNAs in the second lane. (B) RNA gel-blot hybridization, with a digoxigenin-labeled full-length riboprobe for detecting AHVd (+) strands, of the second denaturing gel. Positions of the circular and linear forms of AHVd and CEVd (used as control) are indicated at both sides. Bands between the circular and linear forms could result from UV-induced cross-links, as observed previously in other viroids, while those bands migrating below the linear forms should correspond to degradation products. The circular forms are less abundant than their linear counterparts, a feature also reported for PLMVd and CChMVd. V1 to V4 refer to pairs of small trees from four commercial cultivars ("Esperiega", "Granny", "Verde doncella" and "Brookfield"), respectively, which were AHVd-inoculated and kept in the greenhouse for four months. Notice that in spite of the relatively poor yield of the

nucleic acid preparation from one of the two V2 plants, the AHVd forms were clearly visible by hybridization.

Fig. 3. Primary and proposed secondary structure for the AHVd (+) strand of the "Pacific Gala" reference variant (GenBank MF402932). Changes found in the reference variant (KR506605) of cultivar "Fuji" (Zhang et al., 2014) and in the variant of an apple cultivar co-infected by apple scar skin viroid (Messmer et al., 2017), are denoted with red and blue upper-case characters, respectively. Lower-case characters in black and red denote those changes found in more than one "Pacific Gala" (Messmer et al., 2017; this work) and "Fuji" variants (Zhang et al., 2014), respectively, and changes observed in single variants resulting in co-variations (and conversions of canonical into wobble base-pairs, or vice versa) that did not disrupt the corresponding stems. Symbols (+) and (Δ) refer to insertions and deletions, respectively, and broken lines to the proposed kissing-loop interaction. Inset 1, hammerhead structures of the AHVd plus and minus strands with the nucleotides involved delimited by flags and the self-cleavage sites marked with arrows; black and white symbols refer to plus and minus strands, respectively. Notice that substitutions do not disrupt the stems flanking the central core of 13 nucleotides (boxed) conserved in most natural hammerhead structures of viroid and viroid-like satellite RNAs. Inset 2, slight stem rearrangement in the reference variant of cultivar "Fuji" that leaves unpaired C334 instead of the U333 in the reference variant of cultivar "Pacific Gala". The same numbering is used for both polarities.

Fig. 4. PAGE in a non-denaturing 5% gel of the (+) and (-) monomeric AHVd RNAs (lanes 1 and 3, respectively) resulting from *in vitro* transcription products of linearized plasmids containing head-to-tail dimeric AHVd-DNA inserts. Co-electrophoresis of both RNAs shows a slight difference in mobility indicating that the two RNAs adopt different conformations *in vitro*, with the diffuse appearance of the bands suggesting the existence of more than one conformation in either polarity strand. Lane M, DNA markers with their size in base pairs (bp) indicated. The gel was stained with silver.

A

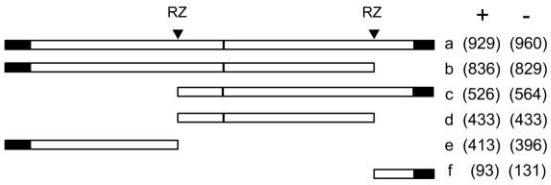

B

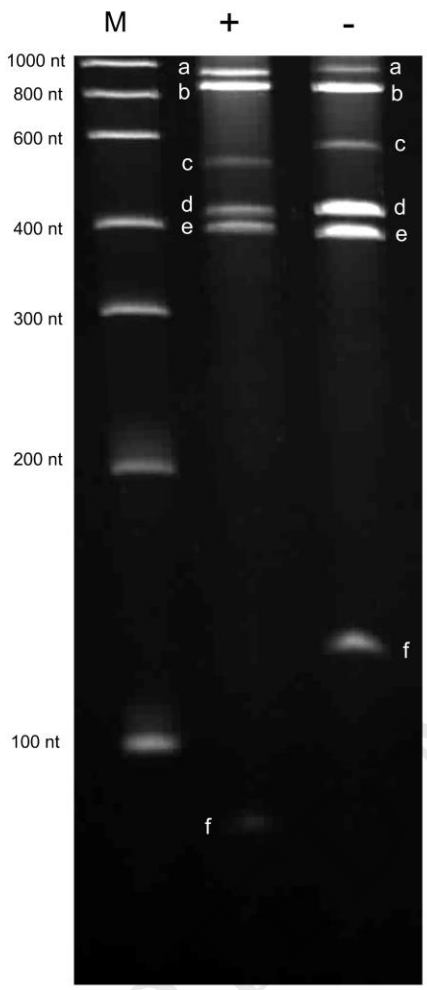

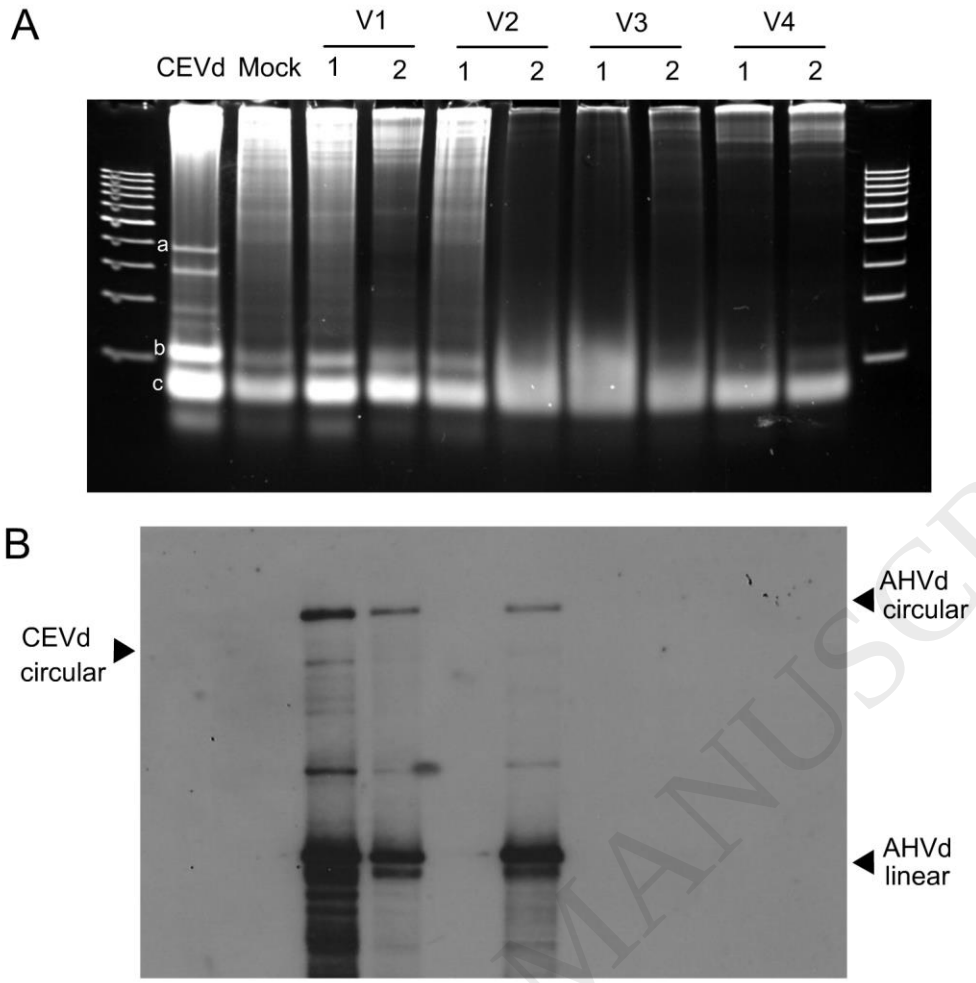

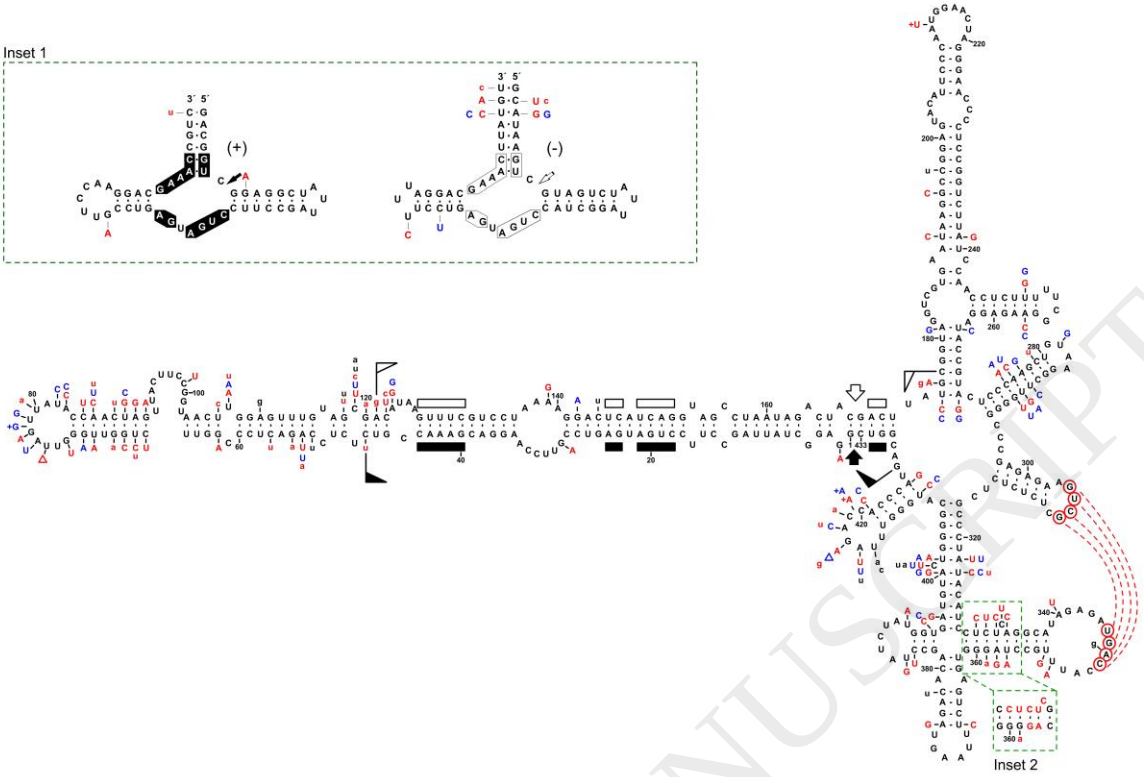

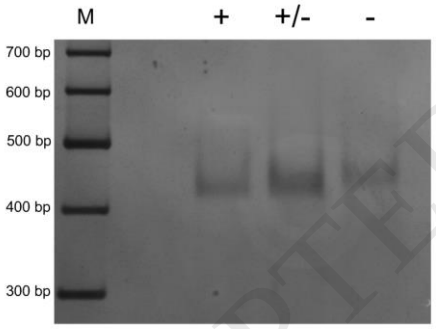

Table 1 AHVd primers for RT-PCR amplification, site directed mutagenesis and subcloning

Primer	Nucleotide sequence	Positions[1]
RF-1379	5´ CTT**R**TCCAACCTCT**K**TTTCGG**M**AGAGGATAC 3´[2]	236-266
RF-1380	5´ ACCGGAGGGGTTCCCTAGTTCC 3´	235-214
RF-1385	5´ AGAGGATGTATAGGGCGAGAGAG 3´	332-310
RF-1386	5′ CAGGCATAGAGATGACCATTTGC 3′	333-355
RF-1388	5′ CAGTCTCTCTCTCGCCCTATACATCCTC 3′	304-331
RF-1389	5′ TTCTCTCGGGCCCCAAGCC 3′	303-285
RF-1390	5´GCTGCATTTGCCTAGGGTGAGTCTTTAAG 3´	345-373
RF-1391	5´ TCTCTATGCCTGAGAGGATGTATAGG 3´	344-319
RF-1422	5´ AGTTGGTATAACTAACCCAACCAGAACC 3´	89-62
RF-1423	5´ AGTTACTTCCGGTAACTTGGAGTTTG 3´	90-115

[1]See Figure 3

[2]**R** denotes A or G, **K** denotes T or G, and **M** denotes A or C